Journal Name

ARTICLE

# Scaling effect on the detachment of pressure-sensitive adhesives through fibrillation characterized by a probe-tack test

Received 00th January 20xx,
Accepted 00th January 20xx

DOI: 10.1039/x0xx00000x

www.rsc.org/

Kosuke Takahashi *[a], Ryuto Oda [b], Kazuaki Inaba [b], and Kikuo Kishimoto [b]

This study extensively investigates the fibrillation process of a pressure-sensitive adhesive (PSA) using a probe-tack test. It was conducted using a glass sphere at the millimeter scale for various thicknesses of PSA layers laminated on a glass substrate, on various contact areas. A sharp decrease in the adhesion force caused by cavity growth was confirmed in the case of large contact areas, whereas cavities were not generated in the case of small contact areas on the thick PSA layer. Furthermore, an atomic force microscopy (AFM) cantilever was used to conduct a probe-tack test on considerably smaller contact areas at the micrometer scale, to focus on the fibrillation process by avoiding the cavity-growth. The transition of the adhesion force during the release process by the AFM cantilever was confirmed to resemble the transition in the fibrillation process obtained using the glass sphere by the repeated tests using the probe without cleaning the surface. The fully adhesive failure was also confirmed by the tests at sufficiently high release velocity. A comparison of these tests at different scales revealed that the detachment force from the probe at the millimeter scale is proportional to the contact area, and determined using the release-strain rate through elongation of the entire thickness of the PSA layer. By contrast, the detachment force from the AFM cantilever is proportional to the contact radius and determined using the release velocity regardless of the PSA thickness.

## Introduction

Pressure-sensitive adhesives (PSAs) are used in our daily life extensively owing to their unique ability to instantly stick to various surfaces and easily detach from the surfaces without leaving remains. Moreover, PSAs do not require a chemical reaction for the adhesive process, whereas structural adhesives must solidify upon bonding; this allows PSAs to retain their flexibility. These characteristics make PSAs particularly suitable for their application in the fields of electronics[1,2] and medical care[3,4]; hence, the demand for PSAs has been increasing. Additionally, PSA products require more severe design, such as bonding on tiny contact areas using very thin PSA layers. To guarantee the reliability of PSA products, the mechanism of adhesion should be clarified such that the products can be designed based on their adhesion strength. However, determining the adhesion strength is difficult because it depends to a great extent on the testing conditions such as the PSA thickness[5–10] and contact area[9,11]. Therefore, it is desirable to develop an evaluation method for quantitatively defining the adhesion strength of PSAs as a material property.

The adhesion force in the release process is typically measured using a peel test and a probe-tack test. In the peel test, the force is measured by peeling one end of the tape attached to the substrates. However, determining the adhesion strength of PSAs as a material property is difficult as the adhesion force is measured according to the deformation of the backing substrate, along with the elongation of the PSA layer itself, and the corresponding adhesion force is distributed[12,13]. A peel test is unsuitable for clarifying the mechanism of adhesion but is suitable for application-based evaluations with respect to specific backing substrates and adherends. By contrast, a probe-tack test measures the transition of the adhesion force from the contact to the release of a probe[14]. Various studies have been conducted to understand this adhesion mechanism since the introduction of the test by Zosel in 1985[15,16]. As the uniform elongation of the PSA layer can be generated through probe displacement and separated from the deformation of backing substrates, this test is suitable for analyzing the adhesion mechanism. Furthermore, the contact area on the PSA layer can be directly observed during the release process[17,18], thereby allowing the correlation between the adhesion force and the deformation behavior[19,20] to be studied. It has been clarified that the adhesion force linearly increases at the beginning, followed by a sharp decrease caused by cavity growth or fingering near the interface. Subsequently, the force gradually increases again owing to fibrillation, until detachment[14,21]. This release process is generally evaluated based on the maximum adhesion stress and the adhesion energy[17].

The maximum adhesion stress for industrial PSAs is typically determined based on cavity-growth[8,22,23], which is caused by the triaxial stress conditions resulting from the tension of the thin PSA layer along the thickness direction[24,25]. In our previous work, we proposed a cavity-growth criterion that successfully characterized the maximum adhesion stress followed by the

[a] Division of Mechanical and Space Engineering, Hokkaido University, N13, W8, Kita-ku, Sapporo, 060-8628, JAPAN. Email: ktakahashi@eng.hokudai.ac.jp
[b] Department. of Transdisciplinary Science and Engineering, Tokyo Institute of Technology, 2-12-1 I6-10, Ookayama, Meguro-ku, Tokyo 152-8552, JAPAN.

fibrillation process[26]. Regardless of the thickness of the PSA layer and the contact pressure, the maximum stress can be predicted by a shape parameter for the effect of confinement —that is the contact radius divided by the thickness of the PSA layer[27,28]—as well as the material properties of the elastic modulus and Poisson's ratio. Furthermore, the maximum stress had a limiting value at the infinite contact radius on zero-thickness; thus, it was defined as an ultimate (ideal) tack strength, which is a material constant representing the adhesion strength.

On the other hand, the adhesion energy has not been quantitatively evaluated because it is assumed to be more difficult due to the significant variations in the fibrillation process. As fibrillation is initiated by cavity expansion, the number of generated cavities and their distribution are assumed to stochastically determine the fibrillation behavior, which affects the adhesion energy directly. To characterize it quantitatively, it is desirable to focus only on the fibrillation process without cavity-growth. When the shape parameter of the contact radius divided by the thickness of the PSA layer is sufficiently small, the generation of cavities can be avoided by decreasing the effect of confinement[27]. Thus, a probe-tack test using an atomic force microscopy (AFM) cantilever is an effective approach to realize a significantly smaller contact area[29,30] for enabling the extraction of only fibrillation during the release process.

This study focused on the fibrillation process during the release process and the detachment of PSAs from the probe surface. In addition to the general probe-tack test using a glass sphere at the millimeter-scale, AFM cantilever was also used for characterizing the fibrillation behavior. In this regard, PSA layers of various thicknesses were prepared to evaluate the effect of thickness on the detachment condition based on various contact areas over different scales from millimeter to micrometer. The adhesion forces at the detachment were measured at various release velocities to quantitatively evaluate the relationship between them.

## Experimental

The PSA layers were prepared by solution polymerization. The acrylate and methacrylate monomers were stirred with azobis (isobutyronitrile) as an initiator and ethyl acetate as a solvent, under nitrogen purging to obtain a copolymer solution. A cross-linker of m-xylylene diisocyanate was then added to the solution. After the solution was cast on a release liner, it was dried at 90°C for 1 min to remove the solvent, and then affixed to glass plates according to their thickness (3–50 μm) using a film applicator. A more detailed preparation and measurement process, using dynamic mechanical analysis (DMA), is described in detail in our previous work[26].

Fig. 1(a) shows the schematic of the probe-tack test. Both edges of the glass plate were clamped, whereby a spherical probe of 6.35 mm was connected to a load cell and actuated using a step motor. Although the contact pressure applied by a spherical probe is not uniform due to its curvature on the contact, the effect on the measurement is negligible if the diameter is

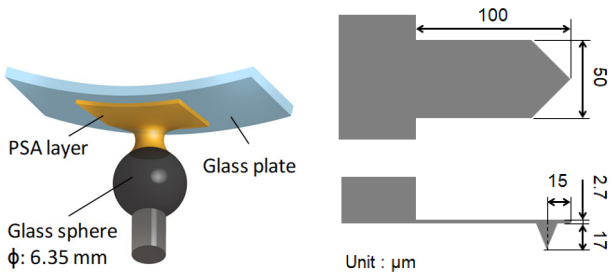


(a) (b)

**Figure 1.** Configurations of probe-tack test using (a) a glass sphere and (b) an AFM cantilever

sufficiently large compared to the PSA thickness. Since a cylindrical probe with a flat surface requires strict alignment to realize uniform contact, a spherical probe is preferable to ensure reproducible measurements for thin PSA layers[26,31–33]. The displaced probe approached the surface of the PSA layer at a fixed velocity of 2.0 μm/s until a specified contact force was reached. This condition was retained for 2 seconds. Subsequently, it was released at a fixed strain rate until complete detachment. In addition to the measurement of the adhesion force during the release process, the probe contact area on the PSA was observed from above using a video microscope to measure the contacting areas. Before each test, the probe surface was carefully wiped with ethanol.

The adhesion performance of the sample was also examined using the tapping mode of AFM (Nanowizard II, JPK). The AFM cantilever was an All-In-One-Al-D (Budget Sensors), which has a 30 nm thick aluminum reflective coating on the detector side of the cantilever. The force constant was 40 N/m. The dimensions are shown in Fig. 1(b). The AFM cantilever was inserted into the sample at an approaching velocity of 0.2 μm/s until the compressive force reached a specified contact force. Subsequently, the AFM cantilever was retracted for detaching from the sample, at a fixed velocity. The force and displacement of the cantilever were measured from the period of contact to detachment. Before each test, the cantilever was blown using a bench top ionizer (ENZR-B, Misumi Corp.) to remove any electrostatic effects. Moreover, the cantilever was carefully cleaned using a UV-ozone cleaner (TC-003, BioForce Nanosciences).

## Results and Discussions

### Probe-tack test using a glass sphere at the mm-scale

The probe-tack test was conducted to sample thicknesses of 5, 15, and 50 μm at a release strain rate of 10 $s^{-1}$ (velocities of 50, 150, and 500 μm/s, respectively) to evaluate the effect of the PSA thickness. Various contact forces from 1 to 100 mN were applied to evaluate the effect of the contact area. Owing to the spherical curvature, the higher the contact forces, the more contact areas there were, and consequently, the higher the adhesion force and the elongation of the PSA layer were, as shown in Fig. 2. Even at the same contact force, a thicker PSA

layer resulted in a higher adhesion force as the probe penetrated deeper with increasing sample thickness, enlarging the contact area.

Fig. 3 shows the images captured using a video microscope under the testing conditions of (a) 1 mN & 5 μm, (b) 100 mN & 5 μm, (c) 1 mN & 15 μm, (d) 100 mN & 15 μm, (e) 1 mN & 50 μm, and (f) 100 mN & 50 μm, respectively. The images were captured at the initial maximum force (i), the end of the sharp decrease (ii), and the maximum force just before detachment (iii). The scale bars in the images represent a length of 100 μm. When the sample thickness was 5 μm, the initiation of cavities, as indicated by the arrows, was observed near the outer edge of the contact area at the maximum force for both 1- and 100-mN contact forces (Figs. 3(a)(i) and 3(b)(i), respectively). Fingering was also observed along the outer edges and in particular, in the case of 100 mN. At the bottom of the force decrease, the cavities were clearly observed to expand, as shown in Figs. 3 (a)(ii) and 3(b)(ii). The number of cavities did not increase until complete detachment, as shown in Figs. 3(a)(iii) and 3(b)(iii), and as reported in our previous study[26]. In the case of the sample of thickness of 15 μm, the initiation of the cavities at the maximum force was more difficult to detect compared to the initiation of the cavities in the sample of thickness of 5 μm. However, fingering along the outer edge of the contact area became clearer, as shown in Figs. 3(c)(i) and 3(d)(i). Although cavity expansion was still confirmed, the number of cavities at the bottom of the force decrease was less, as shown in Figs. 3(c)(ii) and 3(d)(ii). The number of cavities did not increase until detachment, as shown in Figs. 3(c)(iii) and 3(d)(iii). Ultimately, the sample thickness of 50 μm did not exhibit cavity expansion when the contact force was 1 mN, as shown in Fig. 3(e)(i). This was the testing condition of the smallest contact radius divided by the thickness of the PSA layer, which represents the least effect of confinement. As observed in Fig. 2, the force decrement in this testing condition was also minimal. The fingering along the outer edges of the contact area was blunt compared to those in other testing conditions, as shown in Figs. 3(e)(ii)–3(e)(iii). When the contact force was 100 mN the expansion of a single cavity was still observed, as shown in panels (i) and (ii) of Fig. 3(f), which are similar to those for a force of 1-mN and thickness of 15 μm (Fig. 3(c)), until its detachment, as shown in Fig. 3 (f)(iii).

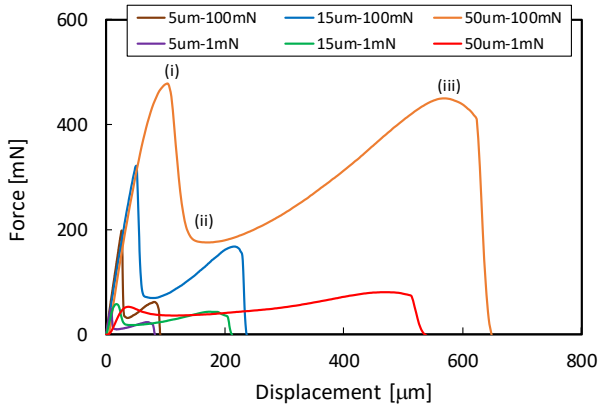


**Figure 2.** Relationship between the force and displacement measured using a glass sphere

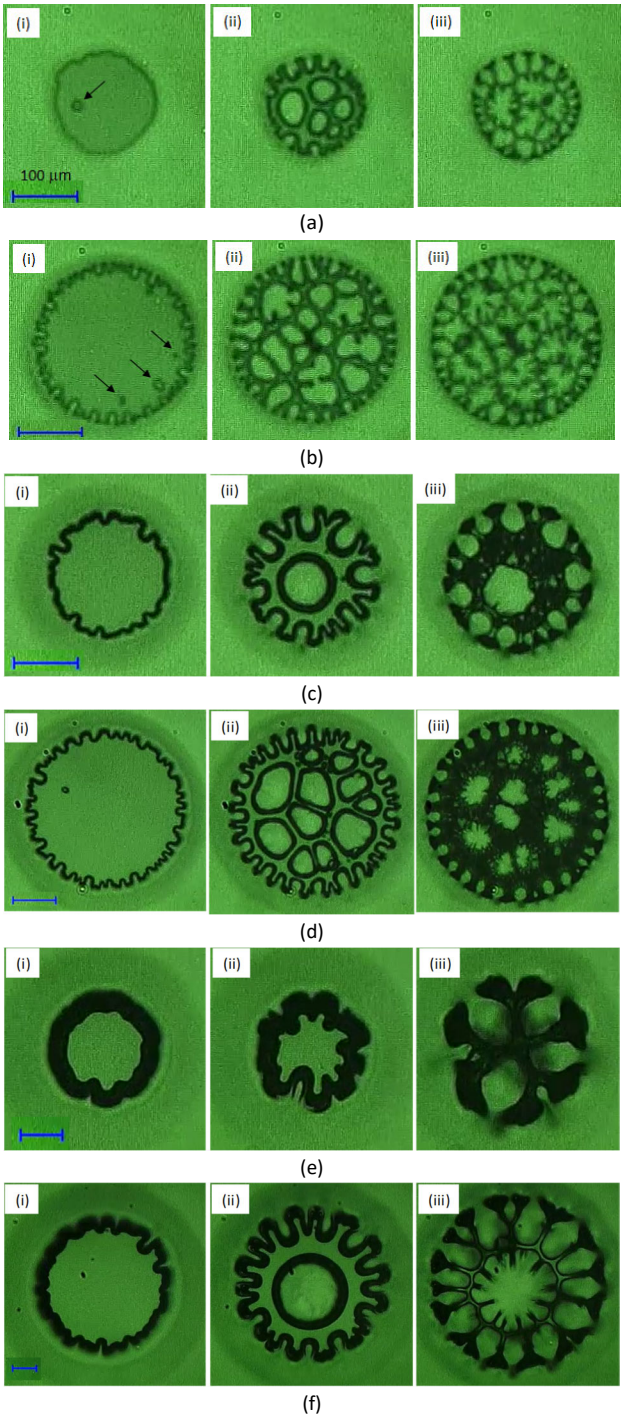


**Figure 3.** Images of contact areas taken at (i) the initial peak, (ii) bottom of sharp decrease, and (iii) the second peak at detachment, indicated in Fig. 2. Testing conditions of the PSA thickness [μm], contact force [mN] are (a) 5, 1; (b) 5, 100; (c) 15, 1; (d) 15, 100; (e) 50, 1; and (f) 50, 100

The force–displacement relation was converted to nominal stress–strain relation to consider the effect of the contact area and the PSA thickness. Fig. 4 plots the adhesion force divided by the contact area, observed using a video microscope, with respect to the displacement divided by the PSA thickness. Note that the displacement of the probe is a sum of the PSA elongation and glass plate deflection. The sharp increment at the beginning appeared to be gentler in the case of a higher contact force of 100 mN owing to the larger deflection of the glass plate. As expected, the thinner samples exhibited higher maximum stress owing to the effect of confinement caused by the higher value of the contact radius divided by the PSA thickness[26]. The clear expansion of cavities in this testing condition also corresponded to the higher maximum stress.

Subsequently, the trends of the bottom of the sharp decrease in the stress curve, as well as the maximum stress just before detachment, were similar in all the cases. This implies that the stress–strain relation during the release process is identical as a material property; there is no effect of confinement on the fibrillation process as the triaxial stress condition is relieved by the expansion of the cavities. Fig. 5 shows the maximum forces immediately before detachment that are summarized in terms of the contact radii, measured for various contact forces from 1 to 100 mN applied to the sample thicknesses of 5, 15, and 50 μm, respectively. In the figure, the square, triangular, and circular markers represent the results obtained from the sample thicknesses of 5, 15, and 50 μm, respectively. The blue, green, and red colors represent strain rates of 10, 4, and 1 $s^{-1}$, respectively. Regardless of the sample thicknesses, the relation between the detachment force and the contact radius was determined according to the release strain rates. It implied that the entire thickness of the PSA layer contributes to the detachment from the probe. As the slope of the data at the same strain rate corresponds to 2, as indicated by the dashed line, the detachment force is proportional to the contact area. Therefore, the detachment can be simply determined using the nominal stress, and there is no need to consider the effect of confinement on the fibrillation process.

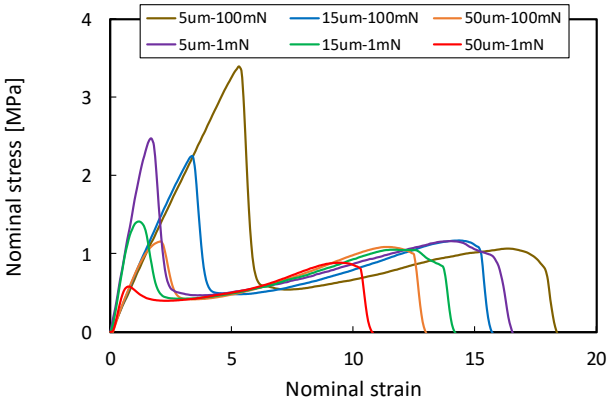


**Figure 4**. Force divided by contact area vs. displacement divided by the PSA thickness, represented as nominal stress–strain relation

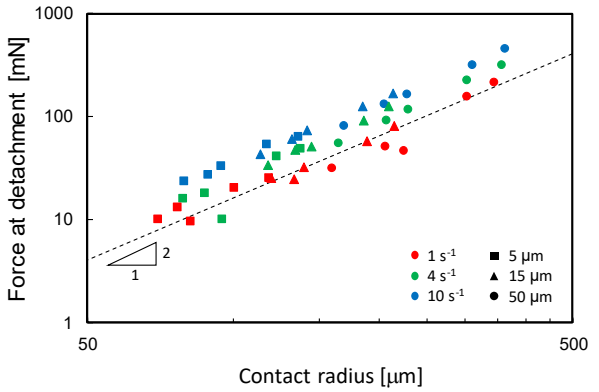


**Figure 5.** Adhesion forces at the detachment, measured according to various PSA thicknesses and contact forces summarized in terms of the release strain rate.

**Probe-tack test using an AFM cantilever at the μm-scale**

The AFM tapping mode was applied to obtain the force–displacement relation for the sample thickness of 3, 5 15, 25, and 50 μm at a release velocity of 0.05, 0,2, and 1.0 μm/s. The contact force was maintained at a constant value of 1000 nN. The test was repeated twice under the same conditions to observe any variations. The cantilever was carefully cleaned after each test.

Fig. 6 shows the results for the sample thickness of 3 15, and 50 μm at the release velocity of 1.0 μm/s. Although variations were apparent in the elongations at the detachment, the maximum adhesion forces were similar regardless of the PSA thickness. The maximum adhesion forces obtained from all the conditions are summarized in Fig. 7. A higher release velocity resulted in a higher maximum adhesion force; however, the sample thickness did not affect this force, even though the strain rate is inversely proportional to the sample thickness. These results indicate that the detachment from the AFM cantilever, wherein the contact radius is far smaller than the PSA layer thickness, is determined locally by the contact condition.

The maximum adhesion forces measured using the AFM cantilever with respect to the contact radius are compared with the detachment forces using the glass sphere. The contact radius of the AFM cantilever was estimated according to the contact depth and angle of the cantilever tip. Fig. 8 shows the results of the AFM cantilever at a release velocity of 1.0 μm/s and those of the glass sphere at a release-strain rate of 10 $s^{-1}$ (velocities of 50, 150, and 500 μm/s for the PSA thickness of 5, 15, and 50 μm, respectively). In addition to the results shown in Fig. 7, tests using the AFM cantilever by the smaller contact forces of 20, 50, 100, 200, and 500 nN were also conducted. The results from the AFM cantilever agree well with a slope of 1, indicating that the detachment was determined by the contact length. By contrast, the results of the glass sphere are in good agreement with a slope of 2, as shown in Fig. 5. Therefore, the probe-tack test using the AFM cantilever was not simply the measurement at a smaller scale, but the contact radius has a significant effect on the detachment force, even though the effect of confinement was negligible on the fibrillation process. It is necessary to examine the failure mode for considering the dependence of the detachment force on the contact radius.

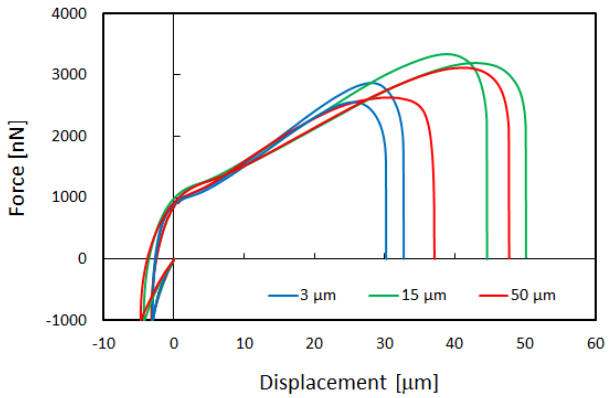


**Figure 6**. Adhesion force and displacement measured using AFM cantilever according to different PSA layer thicknesses

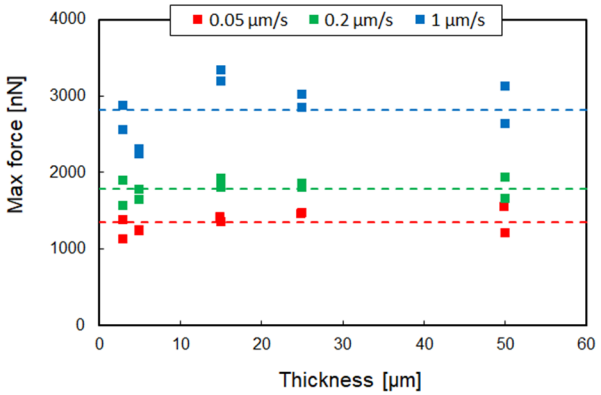


**Figure 7.** Adhesion force at detachment, measured using AFM cantilever according to various PSA layer thicknesses at various release velocities

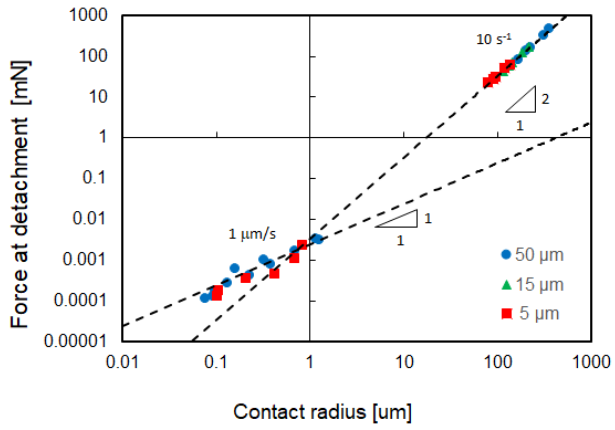


**Figure 8.** Scaling effect of adhesion force at the detachment with respect to the measurements by the glass sphere and AFM cantilever

### Repeated tests without cleaning the probe surface

When the detachment is caused by cohesive failure, the detachment force is determined by the release of the entanglement and extension of molecular chains, which depends on molecular kinetics. These behaviors are macroscopically observed as the viscoelastic property of the tensile strength of the PSA material. When the tensile strength of the PSA material is higher than the strength of the interface between the PSA material and the probe surface, the detachment is caused by adhesive failure.

To investigate the failure modes at the detachment, the probe-tack tests using the glass sphere and the AFM cantilever were repeated without cleaning the probe surface, respectively. If the detachment from the PSA was caused by fully cohesive failure, the probe surface would be completely covered with the fractured PSA material and would result in the significant degradation of the adhesion force in the repeated tests; alternatively, the repeated tests would enable to yield reproducible results by fully adhesive failure because the probe surface remained intact after the repetition.

The results of the repeated tests using the glass sphere are shown in Fig. 9(a). The thickness of the PSA layer was 15 μm, and the strain rate was 10 $s^{-1}$ (velocities of 150 μm/s). The adhesion force on the fibrillation process gradually decreased by repeating the test, and stopped decreasing after the 5$^{th}$ test. This implied that the detachment was mainly adhesive failure at the 1$^{st}$ test, but the PSA material remained on the probe surface slightly and accumulated after every test. Eventually, the contact area on the probe was completely covered with the accumulated PSA material from the previous tests, and the failure mode shifted to fully cohesive failure near the interface after the 5$^{th}$ test. The PSA layer on the substrate plate and the accumulated PSA layer on the probe surface were connected only by the intermolecular force between them, which was unable to sustain the long fibrillation formed by oriented polymer chains. Noticeably, the adhesion force realized from the initial increment to the sharp decrease did not change even after the repetition of ten times, despite the detachment by fully cohesive failure near the interface. This proved that the remains of the PSA material on the probe surface due to previous tests did not affect the growth of cavities; hence, the intermolecular force between the PSA layers could still sustain the condition of cavity-growth.

The results of the repeated tests using the AFM cantilever are shown in Fig. 9(b). The thickness of the PSA layer was 15 μm, and the release velocity was 1.0 μm/s. The contact force was 1000 nN. Although the force–displacement relations were similar until a displacement of 5 μm, the values of the maximum adhesion force and displacement at the detachment obtained in the second test were almost half of the values obtained in the first test. The force and displacement decreased as the number of repetitions increased. However, this decrease at the detachment was no longer observed after the 10$^{th}$ test, as observed using the glass sphere (but after five repetitions). The measurement results reveal that the failure mode at detachment from the AFM cantilever is similar to that from the glass sphere; the detachment is mainly adhesive failure on the clean surface, and gradually shifts to cohesive failure near the interface due to accumulation of the remains on the probe surface at every test.

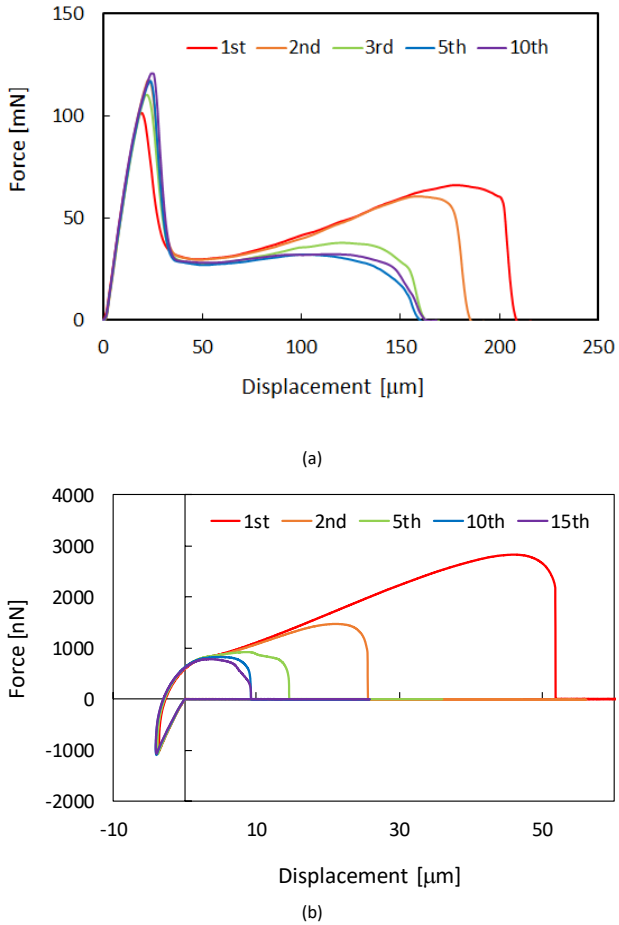


**Figure 9.** Repeated tests without cleaning the probes measured using (a) a glass sphere, and (b) an AFM cantilever

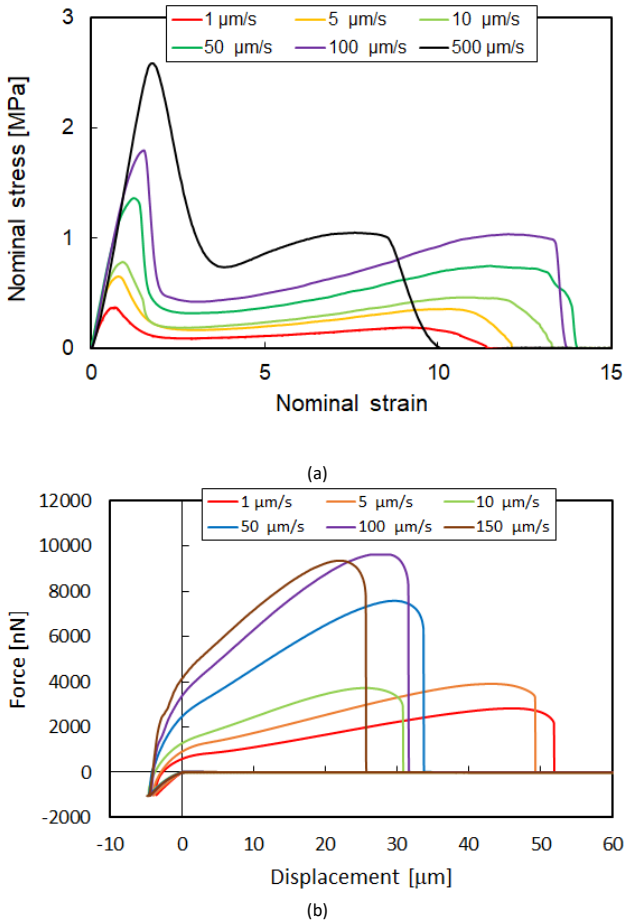


**Figure 10.** Probe-tack tests at higher release velocities to confirm the limiting value of adhesion force at the detachment due to interfacial failure

**Fully adhesive failure at higher release velocity**

The remains of the PSA material on the probe surface could be avoided by the detachment at sufficiently high release velocity because the detachment is expected to be more brittle by the increase in the strength and the stiffness of the PSA materials. Both tests using the glass sphere and AFM cantilever were conducted at even higher release velocities to cause fully adhesive failure. The contact force was fixed at 10 mN and 100 nN when using the glass sphere and AFM cantilever, respectively. The sample thickness was 15 μm. Fig. 10(a) shows the nominal stress–strain curves measured using the glass sphere. The adhesion force increased throughout the release process at higher release velocities up to 100 μm/s, but the detachment stress stopped increasing at 500 μm/s although the initial peak stress still increased. The results of the AFM cantilever are shown in Fig. 10(b) for the same release velocities as those used with the glass sphere. The highest release velocity was 150 μm/s because of the capacity of the AFM. The higher release velocity resulted in a higher maximum adhesion force up to 100 μm/s; however, it did not increase further at 150 μm/s. These results of the adhesion forces were similar to those obtained from the fibrillation process using the glass sphere, although the elongations at the detachment were less dependent on the release velocity. These results indicated that the higher release velocity up to 100 μm/s decreased the remained PSA material on the probe surface at the detachment, and the failure mode shifted to fully adhesive failure at the even higher release velocity. Therefore, the critical adhesion force observed at release velocities higher than 100 μm/s could be regarded as the interfacial strength, which is time independent.

**Detachment conditions from the glass sphere and AFM cantilever**

The detachment from the glass sphere and the AFM cantilever is schematically described in Fig. 11, respectively, based on the gradual decrease of the detachment force by the repeated tests and the critical detachment force at sufficiently high release velocity observed in Fig. 9-10. It should be noted that these detachment behaviors would depend on PSA materials and surface conditions of probes[34].

In the case of the large contact radius using the glass sphere, which is generally larger than the thickness of the PSA layer, the detachment force is determined by the contact area. This normal stress, represented by the distributed arrows in Fig. 11 (left), depends on the strain rate; the elongation of the entire thickness of the PSA layer contributes to the detachment. Although the detachment was confirmed to be mainly adhesive failure, the remains of the PSA material on the probe surface

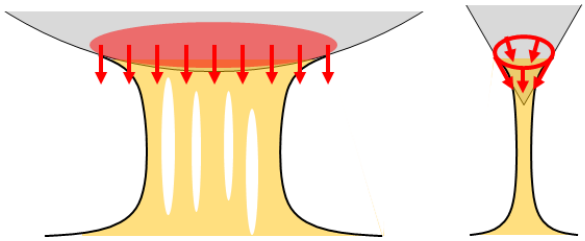

**Figure 11.** Schematic description of the scaling effect determining the detachment by nominal stress by a glass sphere in the millimeter scale (left) and that by surface traction using the AFM cantilever (right)

indicated that the scission of molecular chains also occurred locally near the interface. The interfacial strength by fully adhesive failure at sufficiently high release velocity, as shown in Fig. 10(a), was approximately 1.0 MPa.

When the contact radius becomes sufficiently small using the AFM cantilever, the detachment is determined by the force acting along the contact outline because the detachment was also confirmed to be mainly adhesive failure. It means that shear component of the force is dominant because the force acting along the contact outline directs to the tip of the cantilever, as shown in Fig. 11 (right). Since the high shear stress is expected at the edge of the contact area due to stress concentration, the detachment is determined locally at the contact outline. Therefore, further study is needed to investigate the geometry effect of the probe and relate it to the scaling effect. The strength along the contact line on the interface obtained at sufficiently high release velocity, as shown in Fig. 10 (b), was approximately 0.895 N/m.

## Conclusions

Probe-tack tests were conducted to characterize the detachment of PSAs, based on the fibrillation process. Different scales of the probes were prepared using a 6.35-mm glass sphere and an AFM cantilever, to examine the effects of the scale on the detachment conditions. The following conclusions can be drawn from this study.

The detachment of the glass sphere at the millimeter scale was determined by a nominal stress according to the release–strain rate though the contribution of the entire thickness of the PSA layer. By contrast, the detachment force of the AFM cantilever was proportional to the contact radius according to the release velocity, indicating that the local shear stress along the contact outline determined the detachment.

Repeated tests without cleaning the probe surface led to a gradual decrease in the detachment forces, for both the milliliter-scale glass sphere and the AFM cantilever, thereby indicating that the detachment was mainly adhesive failure, but there were remains of the PSA material on the probe surface. These tests also revealed that cavity growth was not affected by these remains, but the intermolecular forces between the PSA layers on the probe surface and substrate plate could still sustain the condition of cavity-growth.

There is a limiting value of the detachment force for sufficiently high release velocities; this can be identified as the interfacial strength between the probe material and the PSA. Further investigations employing the same material and geometry for probes in the millimeter and micrometer scales will lead to a quantitative characterization of detachment through fibrillation.

## Conflicts of Interest

There are no conflicts to declare.

## Acknowledgements

The preparation of a sample for this work was supported by the Lintec cooperation.

## References


1 C. Creton and E. Papon, *MRS Bull.*, 2003, **28**, 419–423.
2 V. Eveloy, P. Rodgers and M. G. Pecht, *IEEE Trans. Device Mater. Reliab.*, 2004, **4**, 650–657.
3 I. Webster, *Int. J. Adhes. Adhes.*, 1997, **17**, 69–73.
4 J. Li, A. D. Celiz, J. Yang, Q. Yang, I. Wamala, W. Whyte, B. R. Seo, N. V Vasilyev, J. J. Vlassak, Z. Suo and D. J. Mooney, *Science*, 2017, **357**, 378–381.
5 Q. D. Yang, M. D. Thouless and S. M. Ward, *J. Adhes.*, 2000, **72**, 115–132.
6 P. Martiny, F. Lani, A. J. Kinloch and T. Pardoen, *Int. J. Adhes. Adhes.*, 2008, **28**, 222–236.
7 K. Shitajima, N. Karyu, S. Fujii, Y. Nakamura and Y. Urahama, *J. Appl. Polym. Sci.*, 2015, **132**, n/a-n/a.
8 A. Chiche, J. Dollhofer and C. Creton, *Eur. Phys. J. E*, 2005, **17**, 389–401.
9 P. Tordjeman, E. Papon and J.-J. Villenave, *J. Polym. Sci. Part B Polym. Phys.*, 2000, **38**, 1201–1208.
10 K. Takahashi, M. Shimizu, K. Inaba, K. Kishimoto, Y. Inao and T. Sugizaki, *Int. J. Adhes. Adhes.*, 2013, **45**, 90–97.
11 C. Creton and L. Leibler, *J. Polym. Sci. Part B Polym. Phys.*, 1996, **34**, 545–554.
12 D. H. Kaelble and D. H. I\: Aelble, *Cit. Trans. Soc. Rheol. Soc. Rheol. Trans. Soc. Rheol.*, 1965, **9**, 135–163.
13 A. J. Kinloch, C. C. Lau and J. G. Williams, *Int. J. Fract.*, 1994, **66**, 45–70.
14 C. Creton, *MRS Bull.*, 2003, **28**, 434–439.
15 A. Zosel, *Colloid Polym. Sci.*, 1985, **263**, 541–553.
16 A. Zosel, *J. Adhes.*, 1989, **30**, 135–149.
17 H. Lakrout, P. Sergot and C. Creton, *J. Adhes.*, 1999, **69**, 307–359.
18 T. Yamaguchi, K. Koike and M. Doi, *Europhys. Lett.*, 2007, **77**, 64002.
19 C. Creton and M. Ciccotti, *Rep. Prog. Phys*, 2016, **79**, 046601.
20 T. Yamaguchi, C. Creton and M. Doi, *Soft Matter*, 2018, **14**, 6206–6213.
21 A. Zosel, *Int. J. Adhes. Adhes.*, 1998, **18**, 265–271.
22 C. Creton and H. Lakrout, *J. Polym. Sci. Part B Polym. Phys.*, 2000, **38**, 965–979.

23 K. R. Shull and C. Creton, *J. Polym. Sci. Part B Polym. Phys.*, 2004, **42**, 4023–4043.

24 G. H. Lindsey, *J. Appl. Phys.*, 1967, **38**, 4843–4852.

25 Y. Y. Lin, C.-Y. Hui and H. D. Conway, *J. Polym. Sci. Part B Polym. Phys.*, 2000, **38**, 2769–2784.

26 K. Takahashi, Y. Yamagata, K. Inaba, K. Kishimoto, S. Tomioka and T. Sugizaki, *Langmuir*, 2016, **32**, 3525–3531.

27 A. J. Crosby, K. R. Shull, H. Lakrout and C. Creton, *J. Appl. Phys.*, 2000, **88**, 2956–2966.

28 R. E. Webber, K. R. Shull, A. Roos and C. Creton, *Phisical Rev. E*, 2003, **68**, 02185.

29 Y. Sun, B. Akhremitchev and G. C. Walker, *Langmuir*, 2004, **20**, 5837–5845.

30 B. Rajabifar, J. M. Jadhav, D. Kiracofe, G. F. Meyers and A. Raman, *Macromolecules*, 2018, **51**, 9649–9661.

31 A. J. Crosby and K. R. Shull, *J. Polym. Sci. Part B Polym. Phys.*, 1999, **37**, 3455–3472.

32 B. A. Francis and R. G. Horn, *J. Appl. Phys.*, 2001, **89**, 4167–4174.

33 K. Takahashi, M. Shimizu, K. Inaba, K. Kishimoto, Y. Inao and T. Sugizaki, *Int. J. Adhes. Adhes.*, 2013, **45**, 90–97.

34 C. Creton, J. Hooker and K. R. Shull, *Langmuir*, 2001, **17**, 4948–4954.